Association and Surface Properties of a Cyclic Block Copolymer of Ethylene Oxide and Butylene Oxide (Cyclo-B_8E_{42}) in Water

Ga-Er Yu, Zhuo Yang, David Attwood, Colin Price, and Colin Booth*

Manchester Polymer Centre, Departments of Chemistry and Pharmacy, University of Manchester, Manchester M13 9PL, UK

Received May 14, 1996; Revised Manuscript Received August 23, 1996[⊗]

ABSTRACT: A cyclic copolymer of ethylene oxide and 1,2-butylene oxide (cyclo-B_8E_{42}) was prepared by cyclization of triblock copolymer $E_{21}B_8E_{21}$, and its self-association and surface properties were studied by dynamic and static light scattering and surface tension. Critical micelle concentration (cmc), micellar molar mass and size, and molecular areas at the air−water interface were compared with corresponding quantities measured previously for linear triblock and diblock copolymers of similar chain length and composition ($E_{21}B_8E_{21}$ itself and B_8E_{41}). Under similar conditions, the cyclic block copolymer formed larger micelles than the linear triblock but smaller micelles than the linear diblock copolymer. Cyclo-B_8E_{42} and $E_{21}B_8E_{21}$ had similar values of the cmc, about 10 times larger than that of B_8E_{41}.

1. Introduction

Many recent studies of the association and surface properties of oxyethylene/oxypropylene block copolymers [E/P, where E represents an oxyethylene unit (OCH_2-CH_2) and P an oxypropylene unit, $OCH_2CH(CH_3)$] have been based on the commercially available triblock copolymers $E_mP_nE_m$; see, for example, refs 1−3 and references therein. Only two investigations of E/P block copolymers have paid direct attention to the effect of chain architecture on micellization, i.e. comparative studies of copolymers $E_{26}P_{29}$ and $E_{14}P_{30}E_{14}$ in this laboratory[4] and of copolymers $E_{13}P_{30}E_{13}$ and $P_{14}E_{24}P_{14}$ by Zhou and Chu.[5] Recent work in Manchester has been largely concentrated on oxyethylene/oxybutylene copolymers [E/B, where B represents an oxybutylene unit $OCH_2CH(C_2H_5)$] and has included comparisons of linear diblock (E_mB_n) and linear triblock ($E_mB_nE_m$ and $B_nE_mB_n$) copolymers.[6−9] In this paper we describe an extension of that work to include a cyclic block copolymer. Specifically, the copolymers concerned were two linear copolymers, B_8E_{41} and $E_{21}B_8E_{21}$, and a cyclic copolymer, cyclo-B_8E_{42}, made by end-linking the triblock copolymer. The cyclization method was that described previously[10,11] and used for cyclization of a number of polyethylene glycols and for a related triblock copolymer, $E_{72}B_{27}E_{72}$.[12]

Experimental and theoretical studies of the microphase separation of cyclic block copolymers in the bulk state have been reported recently,[13,14] but we know of no report concerning the self-association of cyclic block copolymers in water.

The present work concerns the equilibrium between micelles and unassociated molecules, through measurement of the critical micelle concentration, and the size and extent of association of the resulting micelles, determined by static and dynamic light scattering. Advantage was taken of the endothermicity of the process to promote association by increasing the temperature. Phase separation (clouding) was not a problem in dilute solution, since the copolymer solutions remained clear up to 95 °C. The energetics of micellization require that E/B junctions must lie in the core−fringe interface, so that the cyclic diblock copolymer (cyclo-B_8E_{42}) in the micelle must loop in both core and fringe, whereas the corresponding linear triblock copolymer ($E_{21}B_8E_{21}$) loops only in the core. The cyclic copolymer is similarly conformationally restricted in its unassociated (solution) state. The extent of compensation between these two effects has yet to be determined, and this was a major consideration in planning this study. Additional impetus came from the possibility of using cyclic block copolymers to investigate the properties of adsorbed layers on solid surfaces, since a layer of cyclic copolymer would be composed entirely of loops. Interpretation of the results from such a study would require knowledge of any competing process, such as self-association of the copolymer in solution.

2. Experimental Section

2.1. Gel Permeation Chromatography (GPC). Two GPC systems were used in the work, either three μ-Styragel columns, with porosities 500, 10^3, and 10^4 Å, or three PL-gel columns (two mixed B and one 500 Å). The eluent was THF at 20 °C and 1 cm^3 min^{-1} flow rate. A differential refractometer (Waters R410) was used to detect elution of sample. Elution volumes were referenced to dodecane as internal standard. Calibration was with poly(oxyethylene) standards.

2.2. NMR Spectroscopy. NMR spectra were recorded using either a Varian Unity 500 spectrometer, operated at 500 MHz for ^1H or 125 MHz for ^{13}C spectra, or a Bruker AC300E spectrometer, operated at 300 MHz for ^1H and 75 MHz for ^{13}C spectra. Sample solutions were *ca.* 5 wt % in $CDCl_3$. Assignments were taken from previous work.[10,15]

2.3. Preparation of the Copolymers. The preparation of the two linear copolymers (B_8E_{41} and $E_{21}B_8E_{21}$), by sequential polymerization of 1,2-butylene oxide (systematic name 1,2-epoxybutane) followed by ethylene oxide, has been described in detail elsewhere.[6]

The cyclization of the triblock copolymer followed the general procedure described previously,[10,11] i.e. reaction of copolymer $E_{21}B_8E_{21}$ with dichloromethane (DCM) under Williamson conditions and at high dilution (i.e. the concentration of copolymer $E_{21}B_8E_{21}$ was maintained below 10^{-5} mol dm^{-3}). Under these conditions, ring closure is *via* an acetal linkage, and the formula of the resulting cyclic copolymer (denoted cyclo-B_8E_{42}) can be written schematically as:

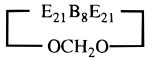

The following reactions are involved:

[⊗] Abstract published in *Advance ACS Abstracts,* November 15, 1996.

S0024-9297(96)00702-4 CCC: $12.00

(i) $-OCH_2CH_2OH + CH_2Cl_2 \rightarrow -OCH_2CH_2OCH_2Cl + HCl$

(ii) $-OCH_2CH_2OCH_2Cl + HOCH_2CH_2O- \rightarrow -OCH_2CH_2OCH_2OCH_2CH_2O- + HCl$

As described below, the conversion of copolymer $E_{21}B_8E_{21}$ to its cyclic counterpart by this route was 85%. This high efficiency reflects the extremely high reactivity of the chloroether formed in step i, which ensures rapid reaction under the conditions of high dilution used to obtain efficient cyclization in competition with chain extension. The chain-extended products could be efficiently removed by fractional precipitation. Conditions under which chain extension can be maximized at the expense of cyclization have been described previously.[16]

In practice, a solution of copolymer $E_{21}B_8E_{21}$ (5 g) in DCM and hexane (100 cm^3) in a syringe pump was slowly added (2 cm^3 h^{-1}) to a stirred suspension of powdered KOH (85%, 7 g) in DCM and hexane (100 cm^3) at 30 °C. The resulting mixture was then stirred for a further 24 h to ensure complete reaction of all hydroxyl groups. The ratio DCM/hexane was 65/35 by volume. Reaction of effectively all OH groups led to the formation of either the required cyclic polymer or extended-chain polymer.

Formation of predominantly cyclo-B_8E_{42} was confirmed by analytical GPC combined with NMR spectroscopy. The GPC method, which has been discussed in several recent publications from this laboratory,[10,11] was based on the shift of elution volume to a higher value when a cyclic polymer is compared with a linear polymer of the same molar mass under otherwise identical conditions.[17] Results for the present reaction are illustrated in Figure 1. A conversion of linear to cyclic copolymer of 85% was estimated from the area under the deconvoluted major peak in the GPC curve of the unpurified reaction product relative to the total area.

An initial purification of the reaction product was effected using the precipitation fractionation procedure developed previously during the preparation of cyclic poly(oxyethylene)s.[10,11,18] The reaction product (*ca.* 5 g) was dissolved in toluene (250 cm^3) at 25 °C. Heptane was slowly added until the stirred solution became cloudy. Equilibrium phase separation was ensured by heating the cloudy solution until it cleared, and then cooling it slowly with gentle stirring to 25 °C. A clear concentrated phase separated from the dilute phase and was removed. Analytical GPC showed that the dilute phase contained cyclo-B_8E_{42} plus a residue of higher-molar-mass copolymer. The separation procedure was repeated, thus reducing but not entirely eliminating the high-molar-mass contaminant. Accordingly, the almost-pure copolymer (*ca.* 3 g) was dissolved in ethanol (10 wt %) and purified by preparative GPC (Sephadex LH-20 gel, two columns each 80 cm long and 2.5 cm diameter, ethanol at 20 °C, flow rate 0.8 cm^3 min^{-1}, differential refractometer detector). The procedure has been described previously.[19] In the present case, a broad center cut of the eluted copolymer was collected. This purified product was isolated by evaporating the solvent, yielding 2.8 g of cyclo-B_8E_{42}, i.e. an overall recovery of 55 wt-%. Its analytical GPC curve (see Figure 1) indicated a narrow chain length distribution: $M_w/M_n \approx 1.05$. The GPC curve of the precursor copolymer ($E_{21}B_8E_{21}$, also shown in Figure 1) indicated a wider (though still narrow) chain length distribution: $M_w/M_n \approx 1.10$. These results are consistent with removal of small fractions of long and short chains by preparative GPC.

^{13}C NMR spectra for the triblock and cyclic copolymers are shown in Figure 2. The spectrum of the purified cyclic product showed resonances from internal oxyethylene carbons (δ = 70.3−70.7 ppm), $\underline{C}H_2$ adjacent to the acetal link (δ = 66.8 ppm), and $\underline{C}H_2$ of the acetal link (δ = 95.5 ppm), with no signals attributable to end groups (61.5 ppm). The integrals confirmed average block lengths (hence average overall molar mass) equivalent to those of the starting copolymer. Considered together, the GPC and NMR results left no doubt that cyclization had been achieved.

The molecular characteristics of the three copolymers considered in the work are set out in Table 1.

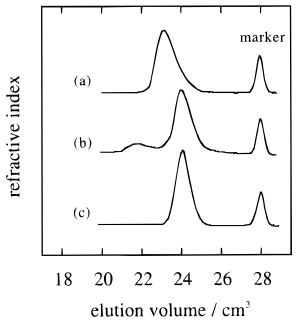

Figure 1. GPC curves for (a) starting triblock copolymer, $E_{21}B_8E_{21}$; (b) cyclization product; and (c) purified cyclo-B_8E_{42}. The system contains three PL-gel columns (two mixed B and one 500 Å). The eluent was THF at 20 °C with a 1 cm^3 min^{-1} flow rate. A differential refractometer (Waters R410) was used to detect elution of sample. Elution volumes were referenced to dodecane as internal standard (marker). Calibration was with poly(oxyethylene) standards.

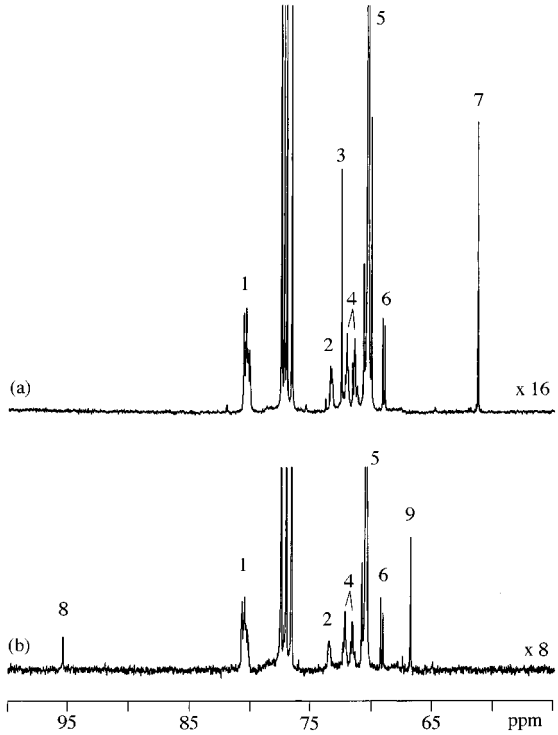

Figure 2. ^{13}C NMR spectra at 75.5 MHz for (a) triblock copolymer, $E_{21}B_8E_{21}$, and (b) cyclo-B_8E_{42} copolymer. Resonances are assigned[10,15] as follows: 1, $-OCH_2\underline{C}H(C_2H_5)$ (B-block backbone); 2, $-(C_2H_5)CH\underline{C}H_2O\underline{C}H_2CH(C_2\underline{H}_5)-$ (initiator residue); 3, $-O\underline{C}H_2CH_2OH$ (E-block end group); 4, $-O\underline{C}H_2CH(C_2H_5)-$ (B-block backbone); 5, $-O\underline{C}H_2\underline{C}H_2-$ (E-block backbone); 6, $OCH_2CH(C_2H_5)O\underline{C}H_2C\underline{H}_2-$ (BE junction); 7, $-OCH_2\underline{C}H_2OH$ (E-block end group); 8, $-OCH_2CH_2O\underline{C}H_2OCH_2CH_2O-$ (acetal link); 9, $-OCH_2\underline{C}H_2OCH_2O\underline{C}H_2CH_2\underline{O}-$ (acetal link).

Table 1. Molecular Characteristics of the Copolymers (NMR and GPC)[a]

copolymer	M_n/g mol^{-1}	M_w/M_n	M_w/g mol^{-1}	wt-% E
$E_{21}B_8E_{21}$	2420	1.1	2660	0.76
cyclo-B_8E_{42}	2420	1.05	2540	0.76
B_8E_{41}	2340	1.1	2570	0.76

[a] Values of M_n and M_w to ±5%.

2.4. Light Scattering. All glassware was washed with condensing acetone vapor immediately before use. Solutions were clarified by filtering through Millipore Millex filters (Triton free, 0.22 μm porosity, sometimes 0.1 μm porosity) directly into the cleaned scattering cell.

Static light scattering (SLS) intensities were measured for solutions maintained at several temperatures in the range 25−50 °C by means of a Malvern PCS100 instrument with vertically polarized incident light of wavelength $\lambda = 488$ nm supplied by an argon-ion laser (Coherent Innova 90) operated at 500 mW or less. The intensity scale was calibrated against benzene. Measurements were made at angles of 45°, 90°, and 135° to the incident beam on solutions at a given temperature over a range of concentration and at 90° at a given concentration over a range of temperature, the latter experiment determining the critical micelle temperature. Dynamic light scattering (DLS) measurements were made under similar conditions by means of the Malvern instrument described above combined with a Brookhaven BI 9000 AT digital correlator. Measurements were usually made at an angle of 90° to the incident beam, but occasionally at smaller angles (30°, 45°). The applicability of these methods to micellar solutions of the type under investigation has been discussed previously.[7,8,20]

The correlation functions from dynamic light scattering (DLS) were analyzed by the constrained regularized CONTIN method,[21] to obtain distributions of decay rates (Γ). Experiment duration was in the range 5−20 min, and each experiment was repeated two to four times. The distributions of decay rates were tested against changes in the regularizer (i.e. prob(α) = 0.25−0.75) and were found to be stable. The decay rates gave distributions of the mutual-diffusion coefficient (D_m) and hence of apparent hydrodynamic radius ($r_{h,app}$, radius of the hydrodynamically equivalent hard sphere corresponding to D_m) *via* the Stokes-Einstein equation

$$r_{h,app} = kT/(6\pi\eta D_m) \quad (1)$$

where k is the Boltzmann constant and η is the viscosity of water at temperature T. The basis for analysis of static light scattering (SLS) was the Rayleigh−Gans−Debye equation, which we write as

$$I - I_s = K^* c M_w \quad (2)$$

where I is the intensity of light scattered from solution relative to that from benzene, I_s is the corresponding quantity for pure solvent, c is the mass concentration, M_w is the weight-average molar mass of the solute, and

$$K^* = (4\pi^2/N_A\lambda^4)(n_B^2/R_B)(dn/dc)^2 \quad (3)$$

where N_A = Avogadro's constant, n_B and R_B = refractive index and Rayleigh ratio of benzene, respectively, and dn/dc = specific refractive index increment. Sources of the quantities necessary for the calculations have been given previously.[20] The value of dn/dc for the present copolymers in aqueous solution at 25 °C was 0.134 ± 0.002 cm^3 g^{-1} and the temperature increment was −0.0002 cm^3 g^{-1} K^{-1}, as obtained previously for aqueous solutions of comparable samples.[22,23]

2.5. Surface Tension. Surface tensions (γ) of dilute aqueous solutions were measured by detachment of a platinum ring suspended from a torsion balance. The usual precautions were taken to ensure cleanliness and the water was doubly distilled and filtered (Millipore Millex-GS, Triton-free, 0.22 μm). The accuracy of measurement was checked by frequent determination of the surface tension of pure water. Solutions were held at the temperature of measurement (40 or 50 ± 0.5 °C) by means of a thermostatted water jacket. The force of detachment was measured after 2 h and at intervals thereafter until consistent readings were obtained. Equilibrium was reached within 2 to 10 h depending on concentration.

3. Results and Discussion

Results for the linear copolymers have been published previously,[6,20] and details are not repeated in this paper. Comparison with results for the cyclic copolymer is made in section 3.6.

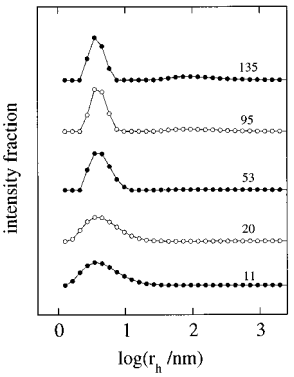

Figure 3. Dynamic light scattering from aqueous solutions of cyclo-B_8E_{42} at 50 °C and concentrations 11, 20, 53, 95, and 135 g dm^{-3} (as indicated). The plots are of intensity fraction of logarithmic apparent hydrodynamic radius, i.e. $I(\log r_{h,app})$ *versus* $\log r_{h,app}$.

There are some problems in making direct comparisons of copolymers with different block architectures. In the case of E/P block copolymers, the anionic polymerization chemistry of propylene oxide is complicated by the transfer reaction,[24] and this can lead to problems of purity in any architectural form. In the case of E/B block copolymers, transfer is not a problem, but the detailed composition of an $E_mB_nE_m$ triblock copolymer (or a B_nE_m diblock copolymer) by sequential copolymerization of butylene oxide followed by ethylene oxide can be affected by the large difference in reactivity of ethylene oxide with E (primary) and B (secondary) oxyanions.[25] This effect leads to E-block length distributions which are wider than is usual in anionic polymerization and, for E-block lengths below 40 units, to a proportion of diblock copolymer in a triblock product.[25] The same effect is important in the preparation of $E_mP_nE_m$ (and P_nE_m) copolymers, but the difference in reactivity of ethylene oxide with primary E and secondary P oxyanions is smaller than that in the E/B system. The composition distributions in the present copolymers had consequences for the investigation of their association and surface properties by light scattering and surface tension methods, but the effects were understood and, as described below, did not form an obstacle to progress.

3.1. Dynamic Light Scattering. Dynamic light scattering (DLS) was used to confirm the extent of micellization in solutions of cyclo-B_8E_{42}, as well as to obtain average values and distributions of hydrodynamic radii. Measurements were made at 25, 35, 45, and 50 °C and for eight concentrations in the range 10−200 g dm^{-3}. Representative intensity−fraction distributions of $\log r_{h,app}$ for solutions of cyclo-$E_{42}B_8$ are shown in Figures 3 and 4.

Considering first the intensity−fraction distributions obtained for solutions at 50 °C (see Figure 3), the peaks at $\log r_{h,app} \approx 0.6$ (i.e. $r_{h,app} \approx 4$ nm) correspond to small micelles. The broader peaks seen for solutions of low concentration probably reflect contributions from molecules (in equilibrium with micelles) which were not resolved by the CONTIN method. Broad weak signals at $\log r_{h,app} \approx 2$ ($r_{h,app} \approx 100$ nm) seen for solutions of moderate concentration gave evidence of scattering from large particles. Since the intensity of scattered light from a given species depends on the product of mass concentration and molar mass through eq 2, the assumption that molar mass is related even approximately to the cube of $r_{h,app}$ leads to the conclusion that the mass concentration of these large particles was very small,

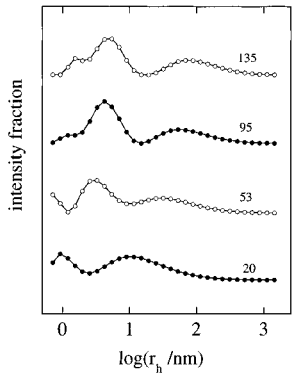

Figure 4. Dynamic light scattering from aqueous solutions of cyclo-B_8E_{42} at 25 °C and concentrations 20, 53, 95, and 135 g dm^{-3} (as indicated). The plots are of intensity fraction of logarithmic apparent hydrodynamic radius, i.e. $I(\log r_{h,app})$ *versus* $\log r_{h,app}$.

e.g. much less than 0.1 wt-% of the solute. It is probable that the particles result from limited micellar aggregation at moderate concentration. The cyclization reaction yields a proportion of chain-extended copolymer, most of which is removed during purification. However, it is inevitable that a fraction of cyclic multiblock copolymer remains in the distribution after purification. This copolymer could give rise to intermicellar links, much as described for triblock copolymer ($B_nE_mB_n$) systems.[20,26] Of course, micellar clustering could have a less specific origin, but no corresponding effect was seen in intensity distributions obtained[6,20] for the linear copolymers considered in this work, i.e. B_8E_{41} and $E_{21}B_8E_{21}$.

The results obtained for solutions at 35 and 45 °C were similar to those illustrated for 50 °C. In the best solvent (25 °C), the intensity−fraction distributions showed an additional signal at low values of $r_{h,app}$ (see Figure 4), providing evidence across the concentration range of molecules ($r_{h,app} \approx 1-2$ nm), micelles ($r_{h,app} \approx 4-5$ nm), and large particles ($r_{h,app} = 50-80$ nm). The greater prominence of the large-particle peaks in Figure 4 (compared to Figure 3) is consistent with a smaller mass fraction of micelles. The argument is based on eq 2. The fact that scattering from unassociated molecules (unimers) is seen in the intensity−fraction distribution implies that they are present in high mass concentration. This in turn implies a much reduced scattering intensity from unimers and micelles together, and hence a relatively high signal from the particles.

Intensity-average values of $r_{h,app}$ were obtained by integrating over the intensity distributions ignoring the large-particle peaks. The extent of micellization at 25 °C was too low for data obtained at that temperature to be treated meaningfully in this way. Plots of $1/r_{h,app}$ against concentration are shown in Figure 5. Through eq 1 this quantity is proportional to $D\eta/T$, and so is compensated for changes in solvent viscosity and temperature. The upturn in $1/r_{h,app}$ at low concentration (<50 g dm^{-3}), seen for all temperatures, is consistent with dissociation of the micelles. The data points at the higher concentrations were linearly extrapolated to obtain values of r_h at infinite dilution for each temperature. These results are listed in Table 2. As can be seen, the hydrodynamic radii of the micelles were small (*ca.* 4.4 nm) and were not greatly dependent on temperature.

3.2. Critical Micelle Temperature and Concentration. Critical micelle temperatures (cmt) were determined for three solutions of copolymer cyclo-B_8E_{42}

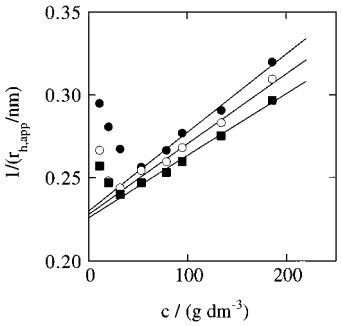

Figure 5. Dynamic light scattering from aqueous solutions of cyclo-B_8E_{42}. Inverse apparent hydrodynamic radius of micelles *versus* concentration for solutions at (●) 35, (○) 45 and (■) 50 °C.

Table 2. Properties of Micelles of Cyclo-B_8E_{42}[a]

T/°C	r_h[b]/nm	δ_h	M_w/g mol^{-1}	N_w	δ_t	r_t
35	4.3	10	20 500	8	1.25	2.1
45	4.4	5.7	40 000	16	1.47	2.8
50[c]	4.4	5.7	40 000	16	1.47	2.8
			(39 000)	(15)	(1.65)	(2.9)

[a] Estimated uncertainties: M_w and N_w, ±15%; r_h, ±5%, r_t, ±10%. [b] Inverse *z*-average value of $1/r_h$. [c] Quantities in parentheses are corrected for scattering from large particles.

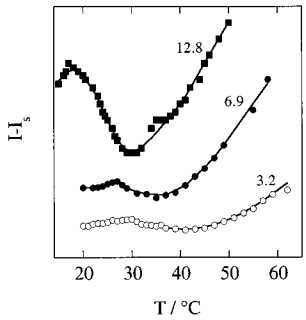

Figure 6. Excess light scattering intensity ($I - I_s$) *versus* temperature for aqueous solutions of cyclo-B_8E_{42} of concentration 12.8, 6.9, and 3.2 g dm^{-3} (as indicated). See section 2.4 for definition of I and I_s.

by measuring the intensity of scattered light as the temperature was raised: see Figure 6. The maxima at low temperatures indicate clouding prior to micellization and are attributable to phase separation of the least soluble species in the composition distribution followed by solubilization when micelles are formed at the cmt. This effect has been seen in the intensity−temperature plots of other E/B copolymers,[6,9] including the triblock precursor ($E_{21}B_8E_{21}$) of the present cyclic copolymer, as well as for $E_mP_nE_m$ copolymers.[4,27,28] Related effects have been described in the distributions of particle size obtained for $E_mP_nE_m$ copolymers by dynamic light scattering.[2,29] As explained previously,[6,9] the cmt was taken to be the temperature at the maximum, giving the values listed in Table 3.

Critical micelle concentrations (cmc) were determined for solutions of cyclo-B_8E_{42} at two temperatures from measurements of surface tension (γ). Plots of γ against the log c are shown in Figure 7. The plots have minima, caused by the presence of highly surface active species in the composition distribution of the copolymer. These are clearly related to those B-rich species which caused the maxima in the intensity−temperature curves. Similar minima have been detected previously for E/B[20,22] and E/P[30,31] copolymers and are known in other surfactant systems.[32] As previously, the cmc was taken to be the concentration at the minimum: see Table 3.

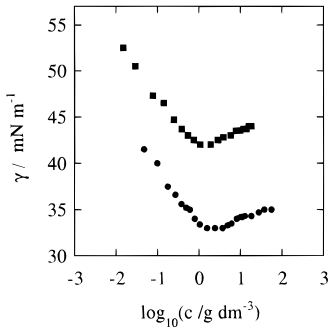

Figure 7. Surface tension *versus* logarithm of concentration for aqueous solutions of cyclo-B_8E_{42} at (●) 40 and (■) 50 °C. For clarity of presentation, the data points for the solutions at 50 °C have been displaced upward by 10 mN m^{-1}.

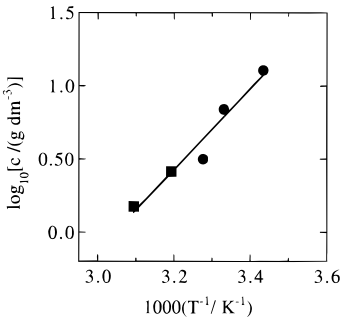

Figure 8. Critical micelle concentrations and temperatures for aqueous solutions of cyclo-B_8E_{42}. Logarithm of concentration *versus* inverse temperature for results obtained from measurements of (■) surface tension (cmc) and (●) light scattering intensity (cmt). The straight line is the least-squares fit to all data points.

Table 3. Critical Temperatures and Concentrations for Cyclo-B_8E_{42} in Water

method	*T*/°C	*c*/g dm^{-3}
light scattering (cmt)	18	12.8
	27	6.9
	32	3.2
surface tension (cmc)	40	2.6
	50	1.5
light scattering (c_{corr})	35	7.5
	45	6.0
	50	5.0

Recognizing that the cmc at a given temperature and the cmt at a given concentration are complementary quantities, the two sets of data in Table 3 are plotted together in Figure 8. The results obtained by the two techniques are seen to be in good agreement. The slope of the least-squares straight line through the points is discussed in relation to the determination of the enthalpy of micellization in section 3.5.

3.3. Micelle Molar Mass. For a nonideal, dilute solution, the Debye equation can be written

$$K^*c/(I - I_s) = 1/M_w + 2A_2c + 3A_3c^2 + ... \qquad (4)$$

where *c* is the concentration of micelles (in g dm^{-3}), M_w is the weight-average molar mass of the micelles, and A_2, A_3, etc. are the virial coefficients which account for the interaction of the micelles in solution. As written, the equation assumes small particles relative to the wavelength of the light. In fact, the value of the dissymmetry ratio was found to be consistently near to unity for the present solutions.

Plots of scattering function $K^*c/(I - I_s)$ against concentration for solutions of cyclo-B_8E_{42} at 35, 45, and 50 °C are shown in Figure 9a. The plots for solutions at 45 and 50 °C are identical within experimental error. As explained above, micellization in solution at 25 °C was limited in extent and a satisfactory Debye plot could not be constructed.

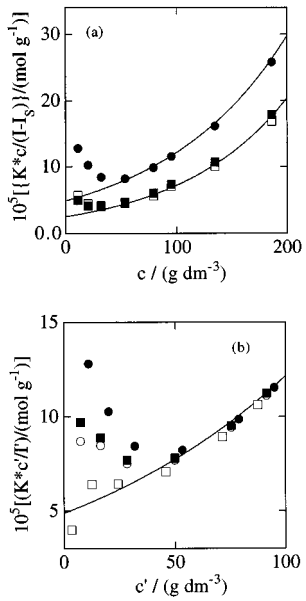

Figure 9. (a) Debye plots for aqueous solutions of cyclo-B_8E_{42} at (●) 35, (□) 45 and (■) 50 °C. Concentrations and intensities are uncorrected. (b) Debye plots for aqueous solutions of cyclo-B_8E_{42} at 35 °C: (●) corrected, $c' = c$, $I' = I - I_s$; (○) corrected, $c' = (c - \text{cmc})$, $I' = I - I_s$; (■) corrected, $c' = (c - \text{cmc})$, $I' = I - I_{cmc}$; (□) corrected, $c' = (c - c_{corr})$, $I' = I - I_s$. The curves were calculated by use of eqs 5 and 6 and are identical in the two graphs. See the text for discussion of the approximations and definition of I_{cmc}. See section 2.4 for definition of K^*, I, and I_s.

Whenever it occurs, and in the absence of other significant effects (e.g. phase separation of the molecular solution at low temperatures), micellar dissociation is made evident by an upturn in the Debye plot at low *c*. This effect was observed at all temperatures studied: see Figure 9a. The Debye function at $c = 0$ for unassociated molecules ($M_w = 2540$ g mol^{-1}) would plot at 40 on the *y*-axis of Figure 9a.

The pronounced curvature of the Debye plots over the full concentration range studied meant that the truncated eq 4 could not be fitted reliably to the data points. This problem was avoided by adopting a suggestion of Vrij[33] and extrapolating from moderate concentrations to zero concentration guided by the Carnahan−Starling equation,[34] which is equivalent to a power series expansion for the structure factor for hard spheres taken to its seventh term. Following this procedure, the interparticle interference factor (structure factor, *S*) in the scattering equation

$$K^*c/(I - I_s) = 1/SM_w \qquad (5)$$

was approximated by

$$1/S = [(1 + 2\phi)^2 - \phi^2(4\phi - \phi^2)](1 - \phi)^{-4} \qquad (6)$$

where ϕ is the volume fraction of equivalent uniform spheres. Values of ϕ were calculated from the actual volume fraction of copolymer in micelles by applying a thermodynamic exclusion factor δ_t, i.e. the thermodynamic volume (v_t) relative to anhydrous volume (v_a), where the thermodynamic volume is one-eighth of the excluded volume. In our treatment, concentrations were

converted to volume fractions assuming a density of dry polymer of $\rho \approx 1.07$ g dm^{-3} irrespective of temperature. Fitting eqs 5 and 6 to the data gave values of M_w and δ_t. Application of above procedure to the scattering intensities obtained for the three copolymers in solution at 25 °C is illustrated in Figure 9a.

Hard-sphere approximations have been used in other laboratories for fitting scattering data from micellar solutions of $E_mP_nE_m$ copolymers (see, for example, refs 35 and 36) and other micellar systems[37] and are firmly rooted in conventional polymer solution theory.[38]

The results were further analyzed using

$$K^*c'/I' = 1/M_w + 2A_2c' + 3A_3(c')^2 + ... \qquad (7)$$

where c' is the concentration of micelles, and I' is the scattering intensity from micelles. Three ways of using eq 7 were considered: (i) $c' = (c - \text{cmc})$ and $I' = I - I_s$; (ii) $c' = (c - \text{cmc})$ and $I' = I - I_{cmc}$, where I_{cmc} is the total scattering from a solution of copolymer (unimer) at its cmc; (iii) $c' = (c - c_{corr})$ and $I' = I - I_s$, with c_{corr} chosen to give an approximately linear extrapolation to zero concentration over the dilute range. In applying option ii, I_{cmc} was equated with $I_s + I_{uni}$, with the excess scattering from unimers (I_{uni}) calculated from eq 2 with $M_w = 2540$ g mol^{-1}. Neglecting the nonideallity of the dilute solution in this way slightly overestimates the value of I_{uni}. Values of the cmc were read off the straight line in Figure 8: i.e. 3.5, 1.8, and 1.5 g dm^{-3} at 35, 45, and 50, °C respectively. Corrected Debye plots for the solutions at 35 °C are shown in Figure 9b: the curve is identical to that shown in Figure 9a. As can be seen, corrections i and ii, which use $c = (c - \text{cmc})$, do not eliminate the upturn at low c. Correction ii differs little from correction i. Indeed, this correction to I has been ignored generally in past practice.

The values of the c_{corr} defined by Figure 9b and similar plots for the data at other temperatures are listed in Table 3. For micellization to a high association number (e.g. >50), the value of c_{corr} should be equal to the cmc. Clearly this condition is not met in the present experiments (see Table 3). Discrepancies between c_{corr} and cmc of a factor of 2 or so have been noted previously for $E_mB_nE_m$ block copolymers.[6,9] The surface tension and cmt methods are designed to detect the early stages of micellization and, to a good approximation, the true cmc is obtained. By contrast, correction of the Debye plot is sensitive to the early stages of dissociation of the micelles. Only if the copolymer composition distribution is very narrow and the micelle association number very high will these two regions relate to the same quantity. In fact, neither of these conditions apply to the present copolymer solutions.

Values of M_w obtained from the intercepts of the plots of Figure 9 are listed in Table 2. Values of the association numbers of the micelles (also listed) were calculated from

$$N_w = M_w(\text{micelle})/M_w(\text{molecule}) \qquad (8)$$

using the value of M_w(molecule) listed in Table 1. Thermodynamic radii, calculated from thermodynamic (equivalent hard sphere) volumes defined as $v_t = \delta_t v_a$, and, for comparison, hydrodynamic swelling factors, defined as the ratio of hydrodynamic volume to dry volume, are also listed in Table 2.

Finally, the effect of the large particles (revealed by DLS, see section 3.1) on the Debye plot was investigated. Scattering from this source led to too-low values of the

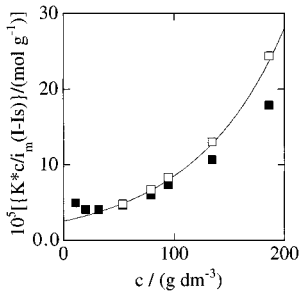

Figure 10. Debye plots for aqueous solutions of cyclo-B_8E_{42} at 50 °C. The data points are either (■) uncorrected ($i_m = 1$) or (□) are corrected for scattering from large particles (i_m given in Table 4). The curve fitting the corrected data at moderate concentration was calculated by use of eqs 5 and 6. See section 2.4 for definition of K^*, I, and I_s.

Table 4. Light Scattering from Aqueous Solutions of Cyclo-B_8E_{42} at 50 °C: Intensity Fraction of Scattering from Large Particles

concn/ g dm^{-3}	fraction of scattering from particles	concn/ g dm^{-3}	fraction of scattering from particles
10.9	0.00	78.9	0.10
19.9	0.00	94.9	0.12
31.7	0.00	134.6	0.18
53.3	0.02	186.0	0.27

Debye function for the more concentrated solutions. Suitable data were available only for solutions at 50 °C. Intensity fractions obtained from the distributions (e.g. from Figure 3), listed in Table 4, were used to correct the Debye plot, as shown in Figure 10. Fitting by the Vrij−Carnahan−Starling procedure gave parameters little different from those obtained from the uncorrected curve: see Table 2.

3.4. Surface Properties. The slope of the plot of surface tension *versus* log c measured below the cmc is related to the excess concentration (Γ) of copolymer in the surface layer (compared to bulk) through the Gibbs adsorption isotherm. For an ideally dilute solution, the Gibbs equation is

$$\Gamma = -\frac{1}{2.303RT}\frac{d\gamma}{d \log c} \qquad (9)$$

If the concentration of solute in solution is negligible compared to its concentration in the surface layer, then the value of Γ gives directly the area per molecule in the surface monolayer, i.e.

$$a = \frac{1}{\Gamma N_A} \qquad (10)$$

Values of the surface area per cyclo-B_8E_{42} molecule were obtained by fitting straight lines to the data points (see Figure 8) below the cmc. The two data sets gave similar values, i.e. an average value of $a = 1.6 \pm 0.2$ nm^2.

A second parameter of interest is the surface tension characteristic of the filled surface monolayer, i.e. the surface tension well beyond the cmc. The results shown in Figure 7 indicate values in the range 34−35 mN m^{-1}.

3.5. Standard Enthalpy of Micellization. If the association number (N) is single-valued (or the average of a narrow distribution of values), then the association equilibrium can be written simply as,

$$A \leftrightarrows \frac{1}{N}A_N \qquad (11)$$

Table 5. Effect of Block Architecture on Micelle and Surface Properties[a,b]

property	cyclo-B_8E4_1	$E_{21}B_8E_{21}$	B_8E_{41}[b]
cmc at 40 °C/g dm^{-3}	3 ± 1	3 ± 1	0.3 ± 0.1
M_w/g mol^{-1}	40000 ± 5000	15000 ± 5000	230000 ± 20000
N_w	16 ± 2	6 ± 2	90 ± 10
r_h/nm	4.4 ± 0.4	4.0 ± 0.5	10
r_t/nm	2.9 ± 0.2	2.2 ± 0.2	7
$\Delta_{mic}H°$/kJ mol^{-1}	55 ± 10	95 ± 20	70 ± 20
a^d/nm^2	1.6 ± 0.3	1.5 ± 0.3	0.64 ± 0.1
$\gamma(c >$ cmc) at 40 °C/mN m^{-1}	35 ± 1	34 ± 1	33 ± 1

[a] Results for linear copolymers $E_{21}B_8E_{21}$ and B_8E_{41} are from references 6 and 20. [b] Aqueous solutions were at 50 °C unless noted otherwise. [c] M_w and r_t were obtained by extrapolation of results for solutions at 20−35 °C. [d] Area per molecule at the air−water interface (from surface tension).

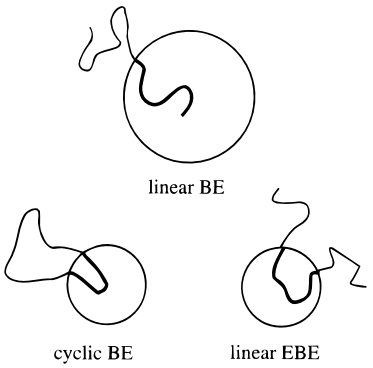

Figure 11. Schematic representation of chain conformations in micelles formed from linear diblock copolymer, cyclic diblock copolymer, and linear triblock copolymer (as indicated).

with the equilibrium constant

$$K = \frac{[A_N]^{1/N}}{[A]} \tag{12}$$

If, in addition, the association number is large (say $N > 50$),[39] then the equilibrium constant $K \rightarrow 1/[A]$ and, taking [A] to be the cmc, the standard Gibbs energy and enthalpy of micellization are given by

$$\Delta_{mic}G° \approx RT\ln(\text{cmc}) \tag{13}$$

$$\Delta_{mic}H° \approx R\frac{\mathrm{d}\ln \text{cmc}}{\mathrm{d}(1/T)} \tag{14}$$

The process referred to is copolymer chains in their standard state of ideally dilute solution at unit concentration (1 mol dm^{-3}) to copolymer chains in their micellar state.

In the case of cyclo-B_8E_{42}, the mass-average association number is small (N ≈ 16; see Table 2). However, even under these circumstances eqs 13 and 14 can give tolerable results. Numerical calculations indicate that $\Delta_{mic}H°$ will be less than 20% in error even though N_w doubles in value over the temperature range considered here. The value of $\Delta_{mic}H°$ calculated directly from the slope of the least-squares straight line in Figure 8 is 55 ± 10 kJ mol^{-1}.

3.6. Effect of Block Architecture. As mentioned above, results suitable for comparison with those presented here for cyclo-B_8E_{42} have been published[6,20] for triblock copolymer $E_{21}B_8E_{21}$ (the precursor in the preparation of the cyclic copolymer) and diblock B_8E_{41}. Selected results are listed in Table 5.

The comparison of interest in the present work is summarized schematically in Figure 11. Compared to the diblock copolymer, both the triblock and the cyclic copolymer are entropically disfavored in the micellar state, the restriction being that two block junctions must be located in the core−fringe interface rather than one. With a given B-block length, as in the present series of copolymers, this restriction also means that the maximum possible radius of a spherical micelle formed from a triblock or cyclic copolymer will be half (or less) that of a micelle formed from the corresponding linear diblock copolymer. Compared to the E blocks of the linear triblock copolymer, the E block of the cyclic copolymer is more conformationally restricted in the micelle fringe. However, because it is similarly restricted in both molecular and micelle states, the effect on the entropy of micellization from this source is likely to be small. The results listed in Table 5 are broadly consistent with these considerations.

Comparing the properties of micelles of the diblock copolymer with those of micelles of the triblock and cyclic copolymers, the ratio of the radii are approximately 2:1 and the ratio of the molar masses (proportional to volume) are approximately 2^3:1. These observations conform to the well-known geometrical requirements for micelles.[40] This aspect has been treated recently as part of a more general theory of micellization of linear block copolymers with different architectures.[41] Extension of the theory to cover cyclic diblock copolymers would be of interest.

Close comparison of the results for cyclo-B_8E_{42} and $E_{21}B_8E_{21}$ (see Table 5) shows that the micellization of the cyclic copolymer is favored over that of the linear triblock copolymer. The principal indicator is the larger association number of the micelles formed from the cyclic copolymer (ratio of values of $N_w \approx 2.7$). The micellar excluded volumes are consistent, i.e. ratio of values of $r_t^3 \approx 2.3$. The hydrodynamic volumes are less sensitive to chain architecture, since the ratio of values of $r_h^3 \approx 1.3$, which could be interpreted as a direct effect of looping in the fringe. However, the results will also be influenced by the small value of N_w of the $E_{21}B_8E_{21}$ micelles, with fewer E-blocks in the micellar fringe forming a more water-swollen structure. A comparison of hydrodynamic volumes for large micelles of cyclic and linear block copolymers based on $E_{72}B_{27}E_{72}$ (N_w in the range 60−80) shows their hydrodynamic volumes to be proportional to their molar masses.[12]

The cmc/cmt data for $E_{21}B_8E_{21}$ available from previous[6] work gives $\Delta_{mic}H° \approx 95$ kJ mol^{-1} compared with $\Delta_{mic}H° \approx 55$ kJ mol^{-1} for cyclo-B_8E_{42} (see Table 5). The lower (positive) value of $\Delta_{mic}H°$ for the cyclic copolymer probably results from reduced exposure of its B_8-block to water when the copolymer is in its molecular state rather than to any effect in the micellar state. The similarity of the cmcs of the two copolymers means there is a smaller standard entropy of micellization for the cyclic copolymer, which is expected considering the

origin of the enthalpic and entropic contributions to the hydrophobic effect.

Acknowledgment. We thank Mr. K. Nixon for help with the GPC. Professor S. W. Provencher kindly supplied a copy of his CONTIN program. Financial assistance came from EPSRC.

References and Notes

(1) Wanka, G.; Hoffmann, H.; Ulbricht, W. *Macromolecules* **1994**, *27*, 4145.
(2) Algrem, M.; Brown, W.; Hvidt, S. *Colloid Polym. Sci.* **1995**, *273*, 2.
(3) Alexandridis, P.; Holzwarth, J. F.; Hatton, T. A. *Macromolecules* **1994**, *27*, 2414.
(4) Yang, L.; Bedells, A. D.; Attwood, D.; Booth, C. *J. Chem. Soc., Faraday Trans.* **1992**, *88*, 1447.
(5) Zhou, Z.-K.; Chu, B. *Macromolecules* **1994**, *27*, 2025.
(6) Yang, Z.; Pickard, S.; Deng, N.-J.; Barlow, R. J.; Attwood, D.; Booth, C. *Macromolecules* **1994**, *27*, 2371.
(7) Yang, Y.-W.; Deng, N.-J.; Yu, G.-E.; Zhou, Z.-K.; Attwood, D.; Booth, C. *Langmuir* **1995**, *11*, 4703.
(8) Yang, Y.-W.; Deng, N.-J.; Zhou, Z.-K.; Attwood, D.; Booth, C. *Macromolecules* **1996**, *29*, 670.
(9) Yu, G.-E.; Yang, Y.-W.; Yang, Z.; Attwood, D.; Booth, C.; Nace, V. M. *Langmuir* **1996**, *12*, 3404.
(10) Yan, Z.-G.; Yang, Z.; Price, C.; Booth, C. *Makromol. Chem., Rapid Commun.* **1993**, *14*, 725.
(11) Yu, G.-E.; Sinnathamby, P.; Price, C.; Booth, C. *Chem. Commun.* **1996**, 31.
(12) Yu, G.-E.; Zhou, Z.-K.; Attwood, D.; Price, C.; Booth, C. *J. Chem. Soc., Faraday Trans.*, in press.
(13) Lescanec, R. L.; Hadjuk, D. A.; Lim, G. Y.; Gan, Y.; Lin, R.; Gruner, S. M.; Hogen-Esch, T. E.; Thomas, E. L. *Macromolecules* **1995**, *28*, 3485.
(14) Marko, J. F. *Macromolecules* **1993**, *26*, 1442.
(15) Heatley, F.; Yu, G.-E.; Sun, W.-B.; Pywell, E. J.; Mobbs, R. H.; Booth, C. *Eur. Polym. J.* **1990**, *26*, 583.
(16) Nicholas, C. V.; Wilson, D. J.; Booth, C.; Giles, J. R. M. *Brit. Polym. J.* **1988**, *20*, 289.
(17) Wright, P. V.; Beevers, M. S. In *Cyclic Polymers*; Semlyen, J. A., Ed.; Elsevier: London, 1986; Ch. 3: H. Höcker, *ibid.*, Ch. 7.
(18) Sun, T.; Yu, G.-E.; Price, C.; Booth, C.; Cooke, J.; Ryan, A. J. *Polymer Commun.* **1995**, *36*, 3775.
(19) Teo, H. H.; Mobbs, R. H.; Booth, C. *Eur. Polym. J.* **1982**, *18*, 541.
(20) Yang, Z.; Yang, Y.-W.; Zhou, Z.-K.; Attwood, D.; Booth, C. *J. Chem. Soc., Faraday Trans.* **1996**, *92*, 257.
(21) Provencher, S. W. *Makromol. Chem.* **1979**, *180*, 201.
(22) Bedells, A. D.; Arafeh, R. M.; Yang, Z.; Attwood, D.; Heatley, F.; Padget, J. C.; Price, C.; Booth, C. *J. Chem. Soc., Faraday Trans.* **1993**, *89*, 1235.
(23) Tanodekaew, S.; Deng, N.-J.; Smith, S.; Yang, Y. W.; Attwood, D.; Booth, C. *J. Phys. Chem.* **1993**, *97*, 11847.
(24) Yu, G.-E.; Masters, A. J.; Heatley, F.; Booth, C.; Blease, T. G. *Macromol. Chem. Phys.* **1994**, *195*, 1517.
(25) Nace, V. M.; Whitmarsh, R. H.; Edens, M. W. *J. Am. Oil Chem. Soc.* **1994**, *71*, 777.
(26) Zhou, Z.-K.; Chu, B.; Nace, V. M.; Yang, Y.-W.; Booth, C. *Macromolecules*, in press.
(27) Zhou, Z.-K.; Chu, B. *Macromolecules* **1988**, *21*, 2548.
(28) Brown, W.; Schillen, K.; Almgren, M.; Hvidt, S.; Bahadur, P. *J. Phys. Chem.* **1991**, *95*, 1850.
(29) Brown, W.; Schillen, K.; Hvidt, S. *J. Phys. Chem.* **1992**, *96*, 6038.
(30) Reddy, N. K.; Fordham, P. J.; Attwood, D.; Booth, C. *J. Chem. Soc., Faraday Trans.* **1990**, *86*, 1569.
(31) Yu, G.-E.; Deng, Y.-L.; Dalton, S.; Wang, Q.-G.; Attwood, D.; Price, C.; Booth, C. *J. Chem. Soc., Faraday Trans.* **1992**, *88*, 2537.
(32) Rosen, M. J. *J. Colloid Interface Sci.* **1981**, *79*, 587.
(33) Vrij, A. *J. Chem. Phys.* **1978**, *69*, 1742.
(34) Carnahan, N. F.; Starling, K. E. *J. Chem. Phys.* **1969**, *51*, 635.
(35) Wanka, G.; Hoffmann, H.; Ulbricht, W. *Colloid Polym. Sci.* **1990**, *268*, 101.
(36) Mortensen, K.; Pedersen, J. S. *Macromolecules* **1993**, *26*, 805.
(37) Brown, R. A.; Masters, A. J.; Price, C.; Yuan, X.-F. In *Comprehensive Polymer Science*; Booth, C., Price, C., Eds.; Pergamon Press: Oxford, U.K., 1989; Vol. 2, Chapter 6.
(38) Flory, P. J. *Principles of Polymer Chemistry*; Cornell University Press: Ithaca, New York, 1953; Chapter 12.
(39) Hall, D. G. In *Nonionic Surfactants: Physical Chemistry*; Schick, M. J., Ed.; Marcel Dekker: New York, 1987; Vol. 23, p 247.
(40) Tanford, C. *The Hydrophobic Effect*; Wiley: New York, 1980.
(41) Linse, P. *Macromolecules* **1993**, *26*, 4437.

MA9607022